Research Article   Open Access

Seismic interpretation of AbuRoash "g" member, in abu gharadig oil and gas field, north western desert, egypt

Ahmed Abdelmaksoud [1], Hatem F. Ewida [2], Galal H. El-Habaak [1] and Ahmed T. Amin [3]

[1] Department of Geology, Faculty of Science, Assiut University, Egypt.

E-mail: ahmed.abdelmaksoud@aun.edu.eg

[2] BP Exploration General Manager in GUPCO, Egypt.

[3] Principle Petrophysicist at RPS Management Consultants, London, UK.

Abstract

Abu Gharadig (AG) oil and gas field lies in the central portion of the AG basin in the northern part of the Western Desert. The Abu Roash "G" (AR"G") represents the basal member of the Abu Roash Formation and comprises shale and limestone with interbeds of sandstone. This member may act as a source, reservoir or seal rock. Structural patterns of the AR "G" Member play an important role in the hydrocarbon potentialities and prospect identification in the area. The data available for the present study include four digital wireline logs, 2D seismic sections, well path data, formation tops and a checkshot survey. The goal of the present study was achieved through the interpretation of the 2D seismic sections using petrel schlumberger modeling software. Two-way time (TWT) and depth structure maps were obtained, in addition to the geo-seismic cross-sections. From the present study, it is concluded that the AR "G" Member suffered compartmentalization by a complex series of normal faults along with anticlinal folding. The anticline has NE-SW axis resulting from NW-SE compression. The fault planes have trends range from EW to NW-SE direction. The fold and the NW-SE faults are of Late Cretaceous age and are related to the time of the positive structural inversion through the AG basin. The fold is asymmetric and doubly plunging. The fold changes its asymmetry and plunging from SW to NE. The normal faults form horsts, grabens and half grabens.

Introduction

In order to find oil and gas accumulations or produce them efficiently once found, then subsurface geology needs to be understood. At its simplest, this means mapping subsurface structure to identify structures where oil and gas may be trapped, or mapping faults that may be barriers to oil flow in a producing field. The seismic method is the most widely used geophysical technique for subsurface mapping [1].

The study area is located between Latitudes 29° 35`N and 30°00`N and longitudes 28° 20`E and 28° 50`E in the AG oil, gas and condensate field which is located in northern part of the Western Desert of Egypt, about 256 Km West of

Cairo and 128 Km South of the Mediterranean coast (Fig.1). The field is located in the central portion of AG basin [2]. The AG basin is a ENE–WSW oriented basin extending for about 300 km long and 60 km wide and represents 3.6% of the Western Desert district [2]. The AG Basin extends between the Qattara Depression to the west and the Kattaniya horst to the east and bounded by two basement uplifts, to the north (Sharib–Sheiba–Rabat platform) and south (Cairo–Bahariya uplift) [3].

The present study aims at subsurface mapping of AR "G" Member and defining the structures affected it through the interpretation of the seismic reflections of this member.

In Badr El Din (BED) concession, the shale interval of AR "G" Member acts as an active seal [4]. The AR "G" Member was evaluated as a good petroleum reservoir in SWS and GPT oil and gas fields in the Abu Sennan area of the north Western Desert [5]. Ferdaus field, in East Abu Gharadig basin, produces oil from the Late Cretaceous sandstones mainly from three reservoirs: Middle, Lower AR "G" members and Upper Bahariya Formation [6]. In different areas of the Western Desert, the AR "G" Member exhibits either a reservoir or source affinity [7]. Thus, the AR "G" Member plays an important role in the hydrocarbon potentialities and prospect identification.

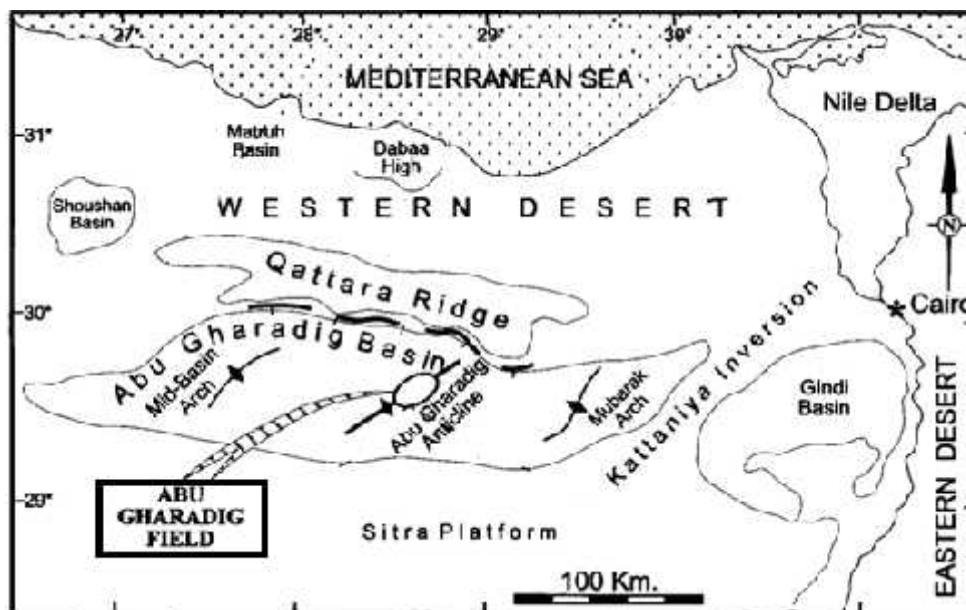

Fig.1; Location map of the AG oil and gas field, Western Desert, Modified after [8].

Geologic Setting

The greater part of the north Western Desert formed a platform characterized by relatively mild subsidence; it was situated near actively subsiding basins or depocenters. The north Western Desert, with the exception of the Abu Roash complex to the north of the Giza Pyramids, is a plateau covered with Neogene sediments [9]. The subsurface lithostratigraphic column of the northern part of the Western Desert comprises a variety of rocks beginning from the Precambrian basement to recent deposits. The thickness of the sedimentary cover overlying the basement rocks reaches more than 35,000 ft in the Abu Gharadig basin, and thins to 9,800 ft over the Ras Qattara ridge at the northern edge of the basin [10]. The oil exploration work including drilling, seismic, gravity and aeromagnetic measurements has revealed the presence of a subsurface stratigraphic column which ranges in age from the Paleozoic to the Recent. The sediments occur in a number of basins with varying degrees of subsidence. The Late Cretaceous succession of the north Western Desert is subdivided into three lithostratigraphic formations (Fig. 2) from the oldest Bahariya, to the Abu Roash and the Khoman Formations [11]. The thickness of the Late Cretaceous succession in Abu Gharadig field is about 7,000ft [10].

The Abu Roash Formation was further subdivided into seven members [12], arranged downwardly as: A, B, C, D, E, F and G. The type section of the Abu Roash Formation is the Mubarak-1 well, where the formation is composed mainly of calcarenite with shale intercalations [2].

The Late Cenomanian AR "G" is the basal member of the Abu Roash Formation which conformably underlies the Abu Roash "F" Member and overlies the Late Albian- Early Cenomanian Bahariya Formation. It is mainly composed of shale, limestone, siltstone and sandstone thin interbeds [5]. Late Cenomanian AR "G" Member is subdivided into upper and lower units. The sandstone development within this member is restricted to the AG Basin and the lower "G" sandstone represents a minor gas pay [13]. Shale beds of the AR "G" Member are considered as a possible source rock, beside the AR "F" which is considered as a fair to excellent source rock, for the siltstone and sandstone reservoirs of the member itself. The shale and limestone of the Abu Roash "G" Member are considered to be the seal rocks, that prevent the upward migration of petroleum accumulated within the member itself [5].

Two main en'echelon normal faults with NE-SW orientation were formed during the Jurassic-Early

Cretaceous time due to NW-SE extension. These faults suffered subsequently positive structural inversion during Late Cretaceous-Middle Eocene time forming the AG anticline. The anticline crest is following the strike of these faults, indicating shortening along NW-SE trend during the Late Cretaceous time. Also, the fold crest suffered compartmentalization by NW-SE oriented normal faults formed parallel to the regional direction of compression causing the inversion. The AG anticline is asymmetric fold and shows changing vergence along the steep NW limb [14]. The present structure configuration of the AG field is a northeast-southwest trending asymmetric faulted plunging anticline.

The anticline along with tilted fault blocks bounded by WNW-ESE and E-W oriented faults, related to the Early Jurassic rift, form the main hydrocarbon traps in the AG field [14].
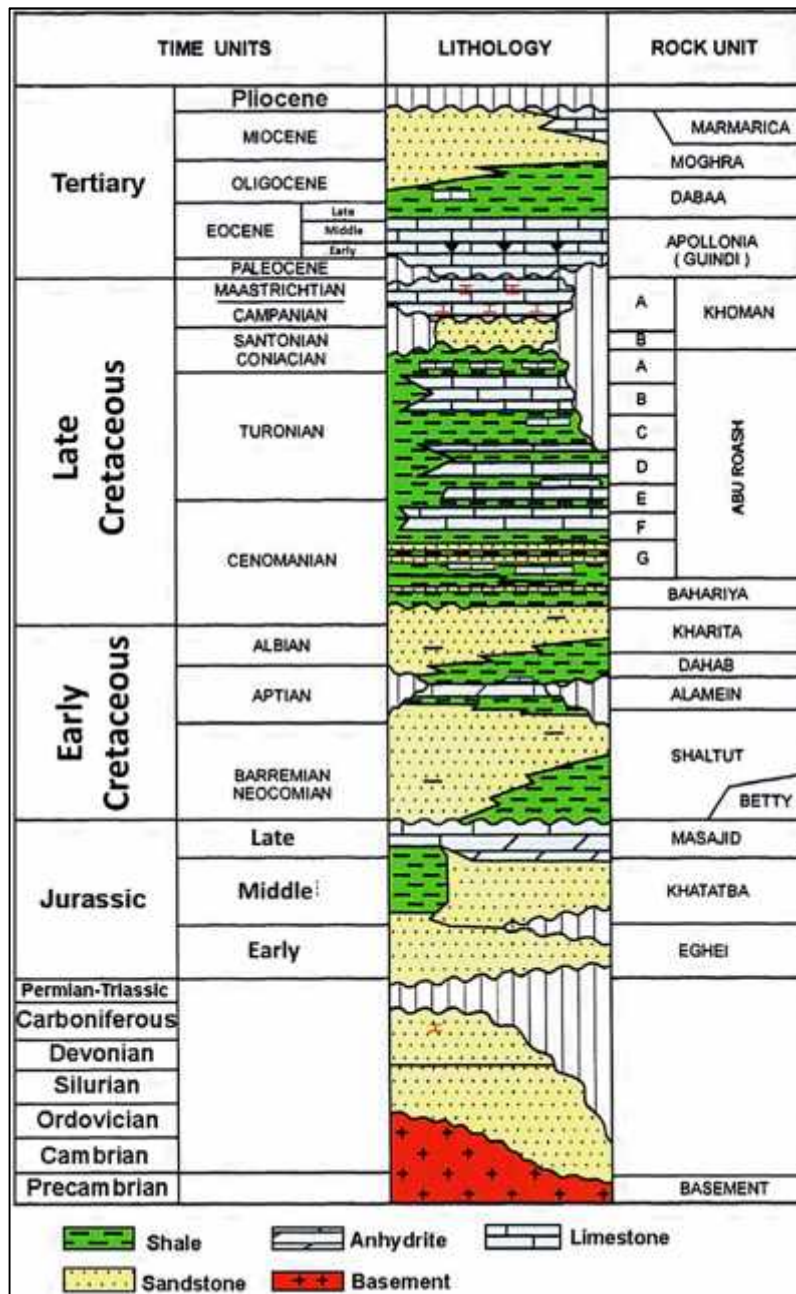

Fig.2; Generalized lithostratigraphic column of the Abu Gharadig basin, modified after [15].

2. Material and Methodology

The available data for the present study were provided by Khalda Petroleum Company after the permission of the Egyptian General Petroleum Corporation (EGPC) (Fig.3). The data include twenty 2D seismic sections, four digital well logs, formation tops and one checkshot survey. The Petrel Schlumberger Modeling Software, version 2013.2, was used in the present study. For achieving the goal of the present study, the following steps were applied to the available data: 1) seismic well tie, 2) picking horizons and interpreting faults, 3) mapping of picked time to construct horizon's two-way time map, 4) domain conversion using velocity map and picked time to construct horizon's depth map, 5) constructing of the geo-seismic cross-sections, and finally 6) the interpretation of the different maps and cross-sections.
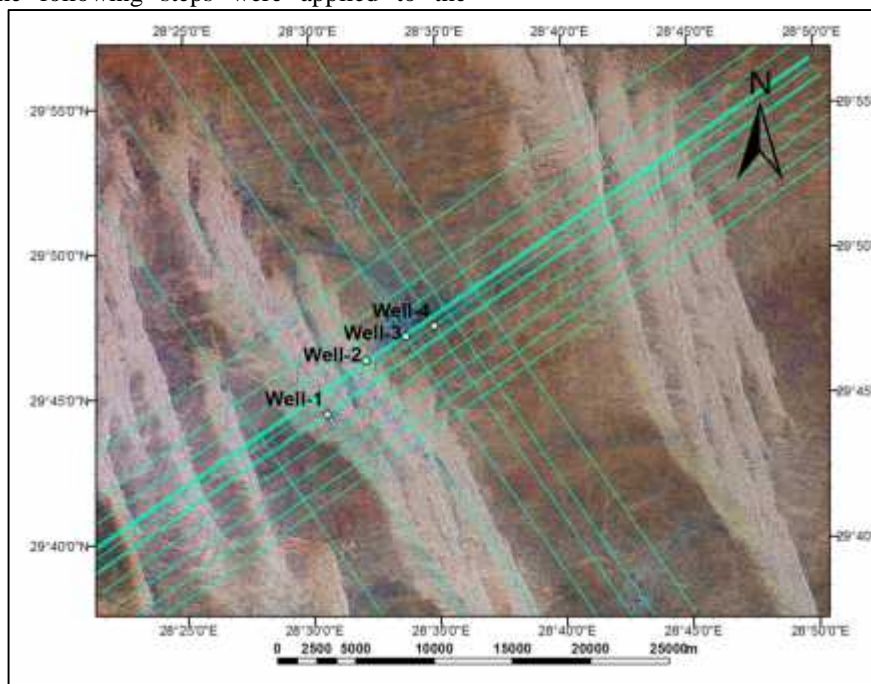

Fig.3; Landsat image [16] with the available wells and seismic lines, AG field.

Seismic to Well Tie

One of the first steps in interpreting a seismic dataset is to establish the relationship between seismic reflections and stratigraphy [1]. Tying well data (in depth) to seismic data (in time) helps to find events (seismic reflections) that correspond to geological formations. There are basically two methods used to tie the geological control into the seismic data: using checkshot data or using synthetic seismogram [17]. The simplest method of tying well data to seismic is to use the checkshot data to convert the tops from depth to time, and post the equivalent horizons on the line at the proper times [18]. In the other hand, the synthetic seismogram is an effective and accurate technique. Often wells will have sonic (i.e. formation velocity) and formation density logs, at least over the intervals of commercial interest, from these it is possible to construct a synthetic seismogram showing the expected seismic response for comparison with the real seismic data [1].

A sonic calibration was performed for the sonic log in well-4 using the available checkshot. The calibrated sonic was used with the density log for determining the acoustic impedance (AI), which is used to define the reflectivity coefficient (RC). For building the synthetic seismogram, a wavelet is needed. Through the wavelet toolbox in petrel, more than one method of determining the wavelet, including; statistical, analytical and deterministic (Extended White) methods, was used and the deterministic method achieved the best fit among them. A synthetic seismogram was built using the generated RC and wavelet (Fig.4). The consistency of the synthetic seismogram with the seismic section is approximately 69%. The formation tops were plotted with the synthetic seismogram and matched with the seismic reflections of inline 5323.
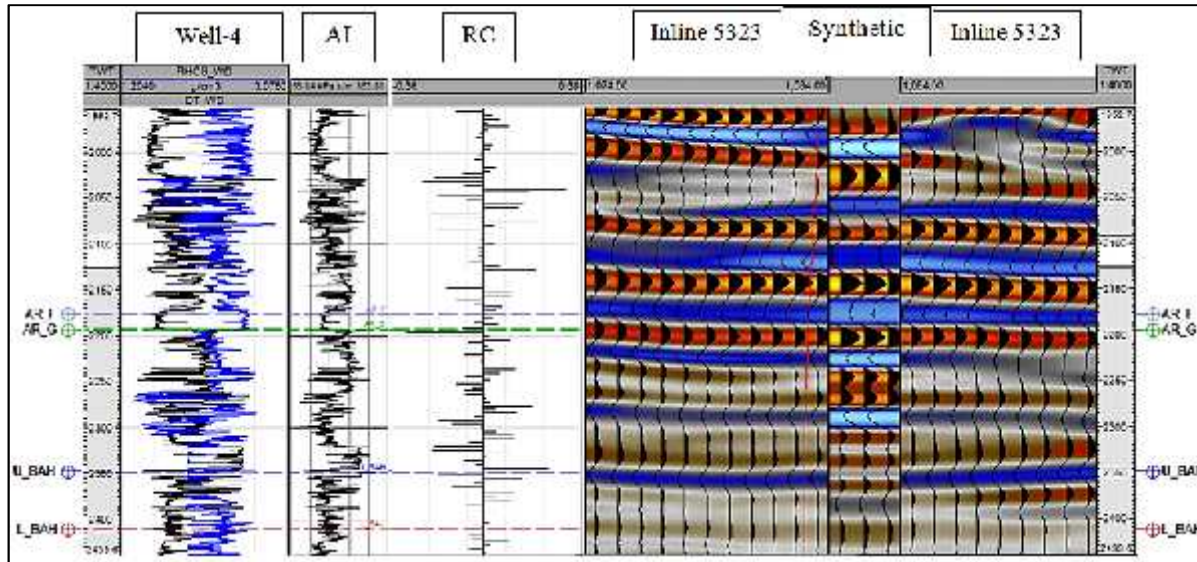
Fig.4; The impedance log (AI), reflection coefficient (RC), and synthetic seismogram generated using the sonic and density logs of well-4; a part of seismic inline 5323 is plotted together with the synthetic seismogram at well-4.

Picking horizons and interpreting faults

It is usually better to start picking reflectors by inspecting seismic sections passing through boreholes. The top of AR "G" Member represents a good event on seismic sections and exhibits a good continuity. The seeded 2D autotracking and the manual interpretation methods were used in the interpretation. In the seeded 2D autotracking method the points will be tracked on the active seismic intersection from the user selected point, and will continue until it does not fulfill the constraints specified in the autotracking tab (e.g. it stops when it comes to a discontinuity or abrupt change in the amplitude value). In manual interpretation, the interpretation is interpolated linearly between picked points. The user defines the end of the segment by double-clicking the left mouse button [19].

The horizons were identified through the tying process and picked along all the seismic lines by correlating the seismic events. The first and the main horizon is the top of AR "G" Member; it is easily visible on the seismic sections and was

easy to be picked. The second one is the top of Upper Bahariya Formation (it is not included in the results, but used with the top of AR "G" Member for constructing the cross-sections); it is not easily visible on seismic sections and was hard to be picked. Thus, due to the low reflectivity of the Upper Bahariya top, it was picked in reference to the top of AR "G" Member (Figs.5, 6, 7, 8). When reflectors are displaced vertically, this interruption may be due to faulting. Faults can be interpreted in 3D, interpretation windows and on any seismic line/display e.g. in-line, cross-line, time slice, random line, arbitrary line, well section fence, etc. [19]. The vertical scale (Z) can be changed to better show the fault displacements. The faults were located and interpreted manually in Petrel software, using the interpret fault tool. Some faults have no continuation on the next seismic sections; while others have more possible continuation. Most of the interpreted faults were located along the in-line direction.
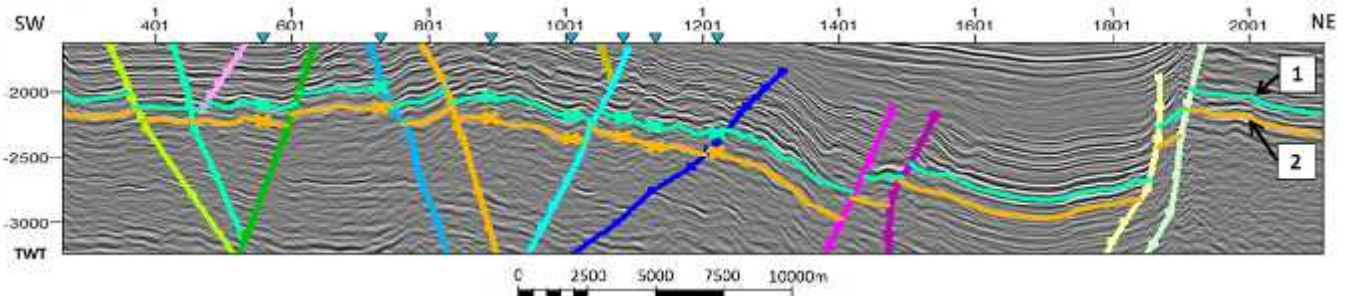

Fig.5: Example of picking the tops of 1) AR "G" Member and 2) Upper Bahariya Formation, and interpreting the faults affecting them (Inline 5300).
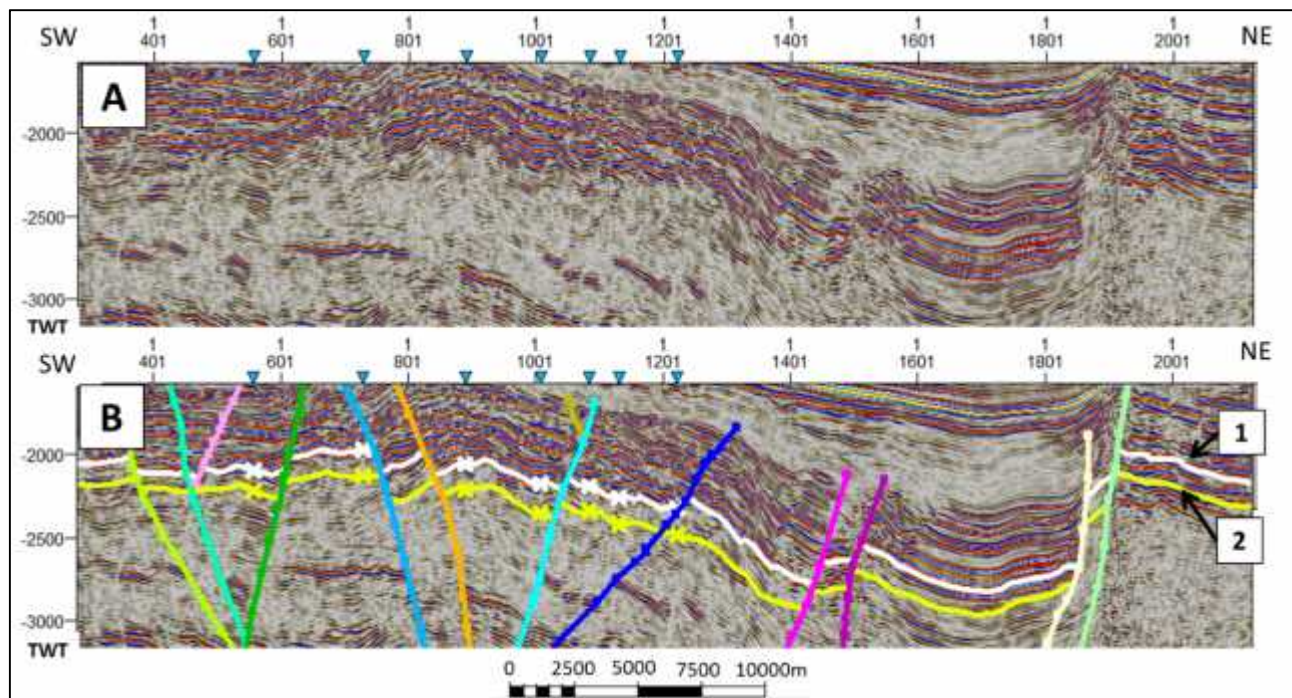
Fig 6: Uninterpreted (A) and interpreted (B) seismic line, inline 5305, where (1) top of AR "G" Member, and (2) Top of Upper Bahariya Formation.
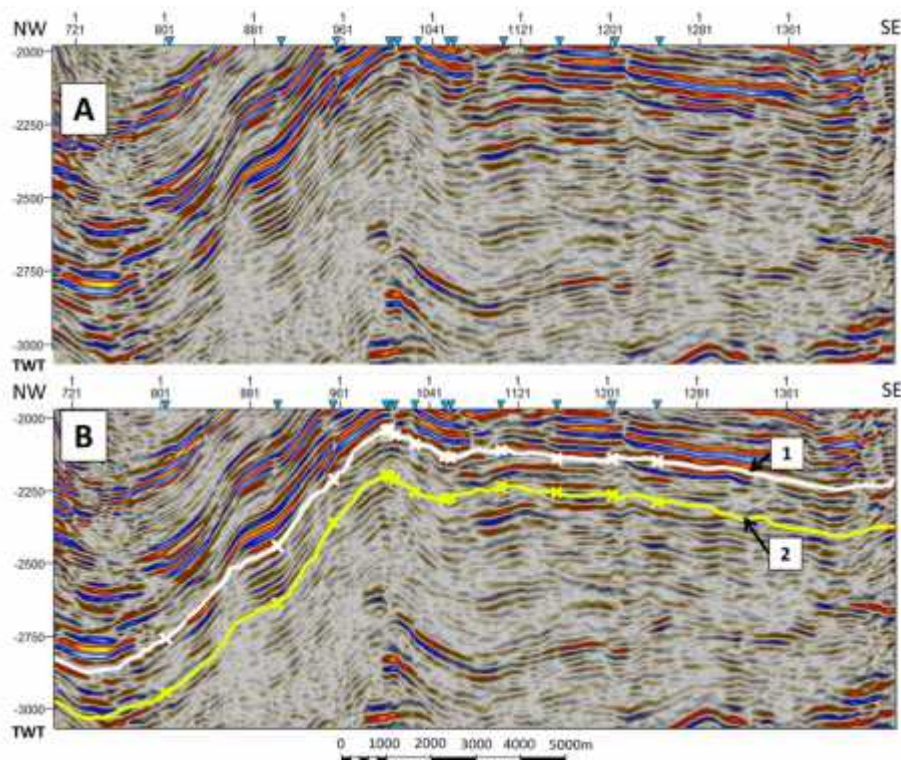

Fig7: Uninterpreted (A) and interpreted (B) seismic line, xline 1718, where (1) Top of AR "G" Member, and (2) Top of Upper Bahariya Formation.
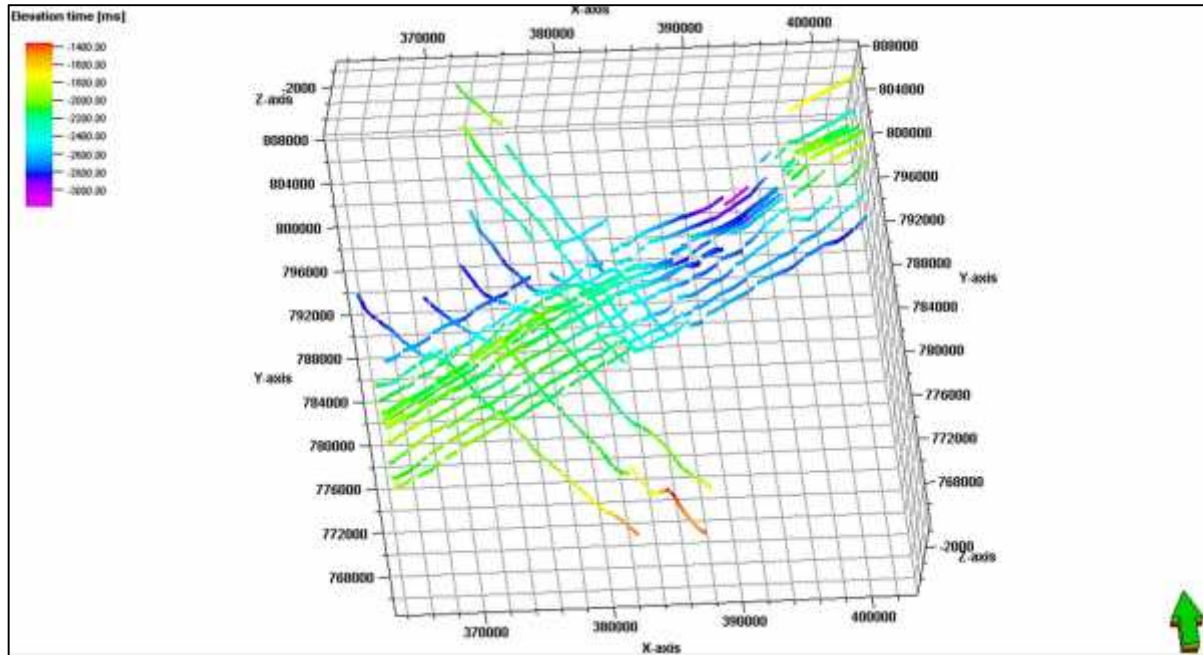
Fig.8; The interpretation lines of top AR "G" Member.

Creating TWT map

After the completion of picking top AR "G" Member and interpreting the faults affecting it, the operation of create fault polygons and map was done on the picked horizon in order to map it or in another word, to make interpolation of the interpretation lines. The generated map is called TWT structure map (Fig.9). The generated fault polygons are not accurate, thus, they were rebuilt manually.
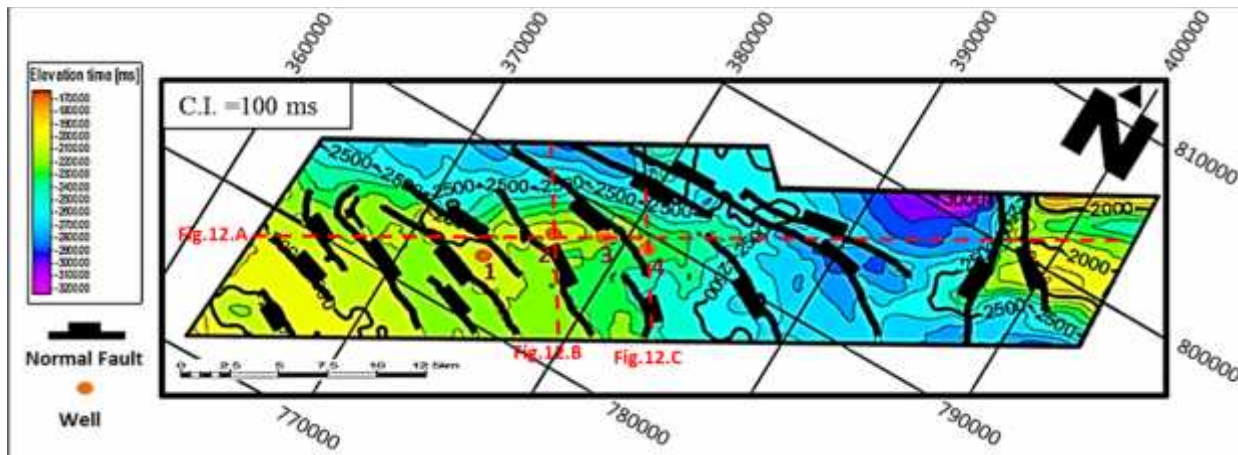

Fig.9; Two-way time structure map of top AR "G" Member.

Time to depth conversion

The physical quantity that relates time to depth is velocity. In most seismic interpretation, it is concerned with the velocity of compressional (P) waves through the earth, because conventional seismic processing attempts to eliminate all seismic energy except that which represents a simple P-wave reflection. The velocity required for converting time to depth is the P-wave velocity in the vertical direction. It can be measured directly in a well, or extracted indirectly from surface seismic measurements, or deduced from a combination of seismic and well measurements [20]. A velocity map for the top of AR "G" was built through the study area (Fig. 10). Then, the velocity map and the TWT map were used to obtain depth structure map for the top of AR "G" Member (Fig.11).
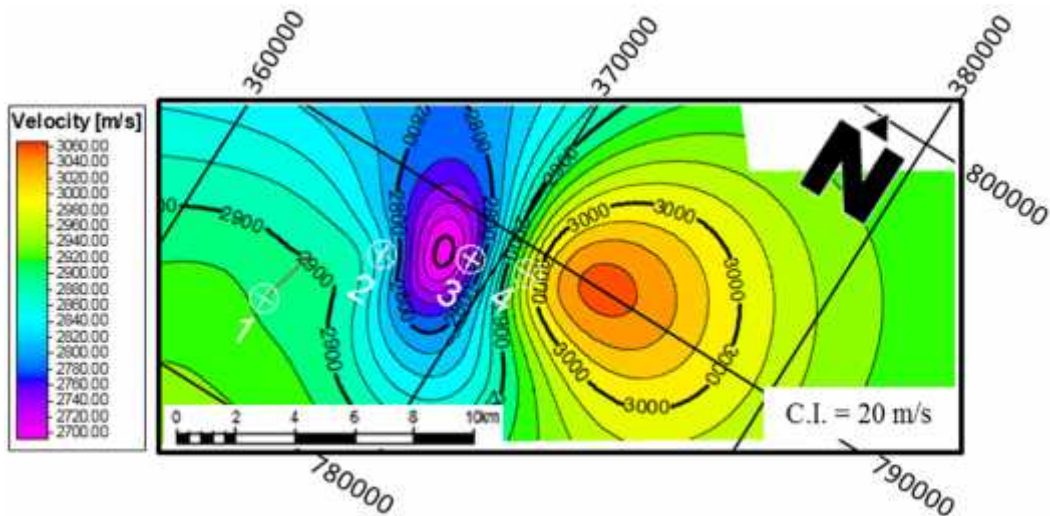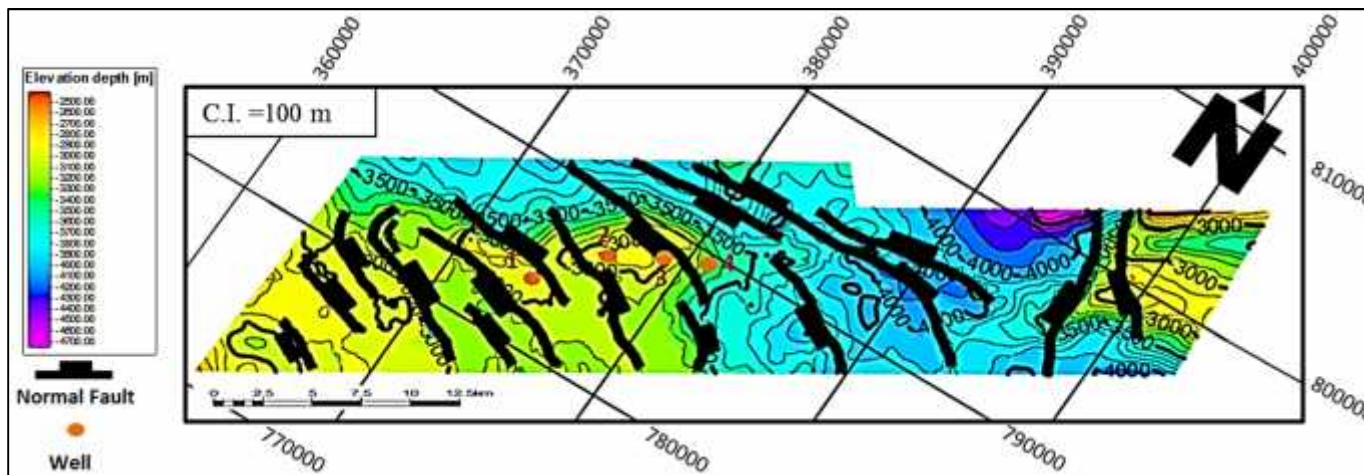
113

Fig10: Velocity map of top AR "G" Member.

Fig.11: Depth structure map of top AR "G" Member.

Construction of seismic cross-sections

To visualize the subsurface structural configuration, geo-seismic cross-sections were constructed to show the structures affecting the AR "G" Member. The cross-sections were constructed automatically through Petrel software using the reconstruction 2D model process with some manual modifications. For these cross-sections, the vertical scale is in TWT and the horizontal scale is defined as meters according the scale bars.
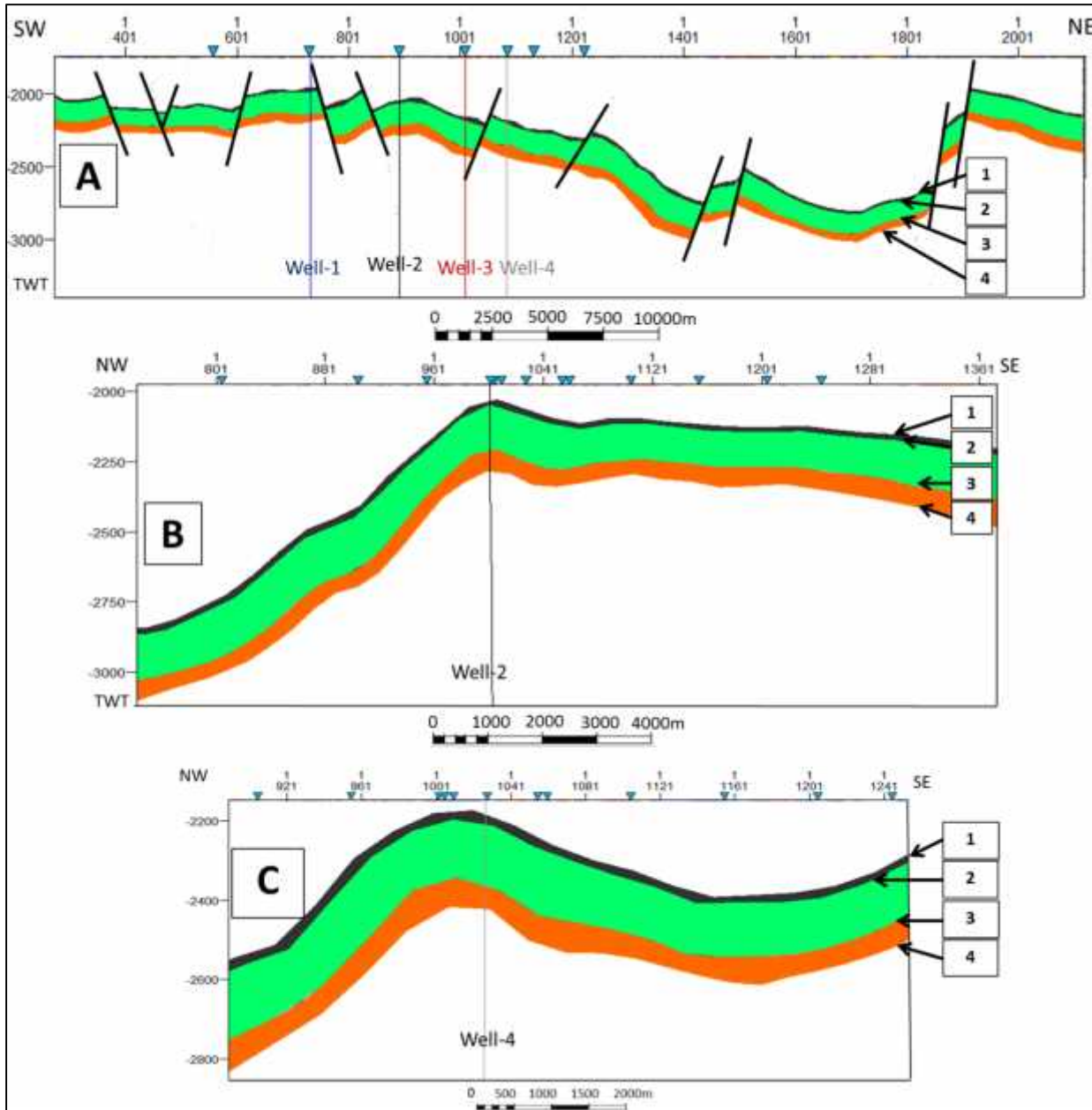
Fig.12: Seismic cross-sections of AR "G" Member through; A) Inline 5305, B) X-line 1718 and C) X-line 1912. Where; 1) Top AR "F", 2) Top AR "G", 3) Top Upper Bahariya, and 4) Top Lower Bahariya Fm. The locations of the cross-sections are shown on Fig.9

3. Results and Discussion

From the seismic cross-sections and maps, it could be stated that the AR "G" Member was compartmentalized by a complex series of normal faults along with anticlinal folding. The anticline has NE-SW axis which suggests that the area was affected by NW-SE compression. The fault planes have trends range from EW to NW-SE direction. The folding and the associated NW-SE faults are of the same age of the Late Cretaceous time and are related to the time of the positive structural inversion through the AG basin. The folding seems to be asymmetric, where along the sides of the anticline the depth contours are not the same; they show a steep NW limb and a gentle SE limb. But, it is clear from contours and the cross-sections (Fig.12.B&C) that the asymmetry of the fold is non-uniform. The steep NW limb changes its angle from less steep at the SW part to more steep in the NE part. Also, the gentle SE limb shows changing from gentle in the SW part to relatively steep in the NE part. The fold is doubly plunging with a gentle plunge to SW and a relatively steep plunge to NE. The cross-sections show that the normal faults form horsts, grabens and half grabens (Fig.12).

115

4. Conclusion

The seismic interpretation passed through the following steps: seismic well tie where a generated synthetic seismogram used in the tying process, picking the tops of AR "G" Member and Upper Bahariya Formation, interpreting the faults affecting them, mapping of picked time to construct horizon's two-way time map, depth conversion using a velocity map and picked time to construct horizon's depth map, and finally the construction of the geo-seismic cross-sections.

It could be concluded that the AR "G" Member was dissected by a complex series of normal faults along with anticlinal folding. The anticline has NE-SW axis suggesting NW-SE compression. The fault planes have trends range from EW to NW-SE direction. The fold and the NW-SE faults are of Late Cretaceous age and they are related to the positive structural inversion through the AG basin. The fold is asymmetric and doubly plunging. The asymmetry and plunging are changed from SW to NE. The normal faults form horsts, grabens and half grabens.

Acknowledgments

References

[1] M., Bacon, R., Simm, and T., Redshaw, 2007, 3-D seismic interpretation, Cambridge University Press, 212 p.

[2] A., Hegazy, 1992, Western Desert oil and gas fields (A comprehensive overview), EGPC 11th Petroleum Exploration and Production Conference, Cairo, p. 1–431.

[3] W., Meshref, M., Abu El Karamat, and M., El Gindi, 1988, Exploration concepts for oil in the Gulf of Suez, *in* Proceedings EGPC 9th Petroleum Exploration and Production Conference, Cairo, Egypt, Volume 1, p. 1-23.

[4] M. A., Ahmed, 2008, Geodynamic Evolution and Petroleum System of Abu Gharadig Basin, North Western Desert, Egypt, Ph.D. Thesis: Institute of Geology and Geochemistry of Petroleum and Coal, RWTH-Aachen University, Germany, 255 p.

[5] M. A., Abd Elhady, T. A., Hamed, and M. A., Abdelwahhab, 2014, A new hydrocarbon prospect determination through subsurface and petrophysical evaluation of Abu Roash "G" Member in Abu Sennan area, north Western Desert, Egypt: Nature and Science, v. 12, no. 11, p. 199-218.

[6] A., Mira, W., Meshref, A. M., Radwan, A., Mostafa, A., Rayan, M., Hassanin, and A., Saad, 2015, Structural, stratigraphic geology and pressure compartmentalization of feradus field based on 3-D seismic data and subsurface geology, *in* Proceedings Society of Petroleum Engineers - SPE North Africa Technical Conference and Exhibition, NATC, p. 1540-1565.

[7] S. S., Tahoun, and A. S., Deaf, 2016, Could the conventionally known Abu Roash "G" reservoir (upper Cenomanian) be a promising active hydrocarbon source in the extreme northwestern part of Egypt? Palynofacies, palaeoenvironmental, and organic geochemical answers: Marine and Petroleum Geology, v. 76, p. 231-245.

[8] K., Khaled, 1999, Cretaceous source rocks at the Abu Gharadig oil-and gas field, northern Western Desert, Egypt: Journal of Petroleum Geology, v. 22, no. 4, p. 377-395.

[9] G., Hantar, 1990, Chapter 15; North Western Desert, In: R. Said (Ed.), The geology of Egypt: Rotterdam; Brookfield, Published for the Egyptian General Petroleum Corp., Conoco Hurghada Inc. and Repsol Exploration, S.A. by A.A. Balkema, p. 293-319.

[10] Schlumberger, 1995, Well Evaluation Conference, Egypt. Schlumberger Technical Editing Services, Chester., p. 356.

[11] B., Issawi, M., El-Hennawy, M., Francis, and A., Mazhar, 1999, Geological interpretation of the main geomorphic units in Egypt: Phanerozoic Geol. Egypt, Geodynamic Approach, Spec. Publ., no. 76.

[12] A., Aadland, and A., Hassan, 1972, Hydrocarbon potential of the Abu Gharadig basin in the Western Desert, Egypt, 8th Arab Petrol. Cong., Algiers: Paper No. 81, (B-3), p. 19.

[13] M., Ezzat, and M., Dia El-Din, 1974, Oil and gas discoveries in the Western Desert-Egypt (Abu Gharadig and Razzak fields): 4th Exploration Seminar, EGPC, Cairo, p. 1-16.

[14] A. M., El Gazzar, A. R., Moustafa and P., Bentham, 2016, Structural evolution of the Abu Gharadig field area, Northern Western Desert, Egypt: Journal of African Earth Sciences, v. 124, p. 340-354.

[15] M., Mahsoub, R., Abulnasr, M., Boukhary, M., Faris, and M., Abd El Aal, 2012, Bio-and Sequence Stratigraphy of Upper Cretaceous–Palaeogene rocks,

East Bahariya Concession, Western Desert, Egypt: Geologia Croatica, v. 65, no. 2, p. 109-138.

[16] MDA Federal, 2004, Landsat GeoCover ETM+ 2000 Edition Mosaics Tile N-35-25. ETM-EarthSat-MrSID, Version 1.0, USGS, Sioux Falls, South Dakota.

[17] M. E., Badley, 1987, Practical Seismic Interpretation: The Journal of the Acoustical Society of America, v. 82, no. 3, p. 1100-1100.

[18] D. J., Tearpock, and R. E., Bischke, 2003, Applied subsurface geological mapping, Upper Saddle River, New Jersey, Pearson Education, 822 p.

[19] Schlumberger, 2007, Petrel Introduction Course, Norway, Schlumerger, 559 p.

[20] A. R., Brown, 2004, Interpretation of Three-dimensional Seismic Data, Tulsa, Oklahoma, U.S.A., AAPG Memoir 42, SEG Investigations in Geophysics, No. 9, 534 p.

[21] M. L., Keeley, and R. J., Wallis, 1991, The Jurassic System in northern Egypt: II. Depositional and tectonic regimes: Journal of Petroleum Geology, v. 14, p. 49-64.